forum acusticum 2026
8-12 September · Graz, Austria

EXPLORING GRAZ BY TRAM: MONITORING THE NETWORK USING VIBRO-ACOUSTIC ONBOARD SENSORS

Karoline Alten[1], Andreas Hula[1], Andreas Fuchs[1], Thomas Huber-Deutsch[2]

[1] *AIT Austrian Institute of Technology GmbH, Center for Transport Technologies, Vienna, Austria*
[2] *Holding Graz - Kommunale Dienstleistungen GmbH, Graz, Austria*

Abstract

Onboard measurement systems installed on rail-bound vehicles have emerged as an effective means of monitoring the interaction between rolling stock and track infrastructure under real operating conditions. Deployed on in-service passenger vehicles or dedicated inspection units, these systems typically integrate multiple sensing technologies. The present study investigates the application of vibro-acoustic sensors mounted below the primary suspension of tram vehicles to characterise emission behaviour over a monitoring period exceeding one year. The analysis is based on data collected during a transnational research initiative across Austria, Germany and Switzerland, focusing on measurements from three in-service tram vehicles operating on the standard-gauge network in Graz. The sensor configuration comprised microphones with direct line-of-sight to the wheel–rail contact point and accelerometers mounted on the axle boxes of both front wheels of the central, unpowered bogie.

The analysis identifies characteristic vibro-acoustic signatures associated with different wheel–rail contact conditions, including faults and regular infrastructure components such as crossings, switches and expansion joints, while highlighting statistically significant network-wide trends. Particular emphasis is placed on processing measurements acquired under highly variable operating conditions. The study demonstrates the potential of advanced signal processing techniques to extract meaningful infrastructure condition information from large-scale, long-term datasets, supporting condition monitoring strategies for urban rail systems.

Keywords: *vibro-acoustic emissions, lightrail vehicles, condition monitoring*

Corresponding author: *karoline.alten@ait.ac.at.*

1. Introduction

This study investigates the use of vibro-acoustic sensors installed below the primary suspension of trams to analyse network-wide emission behaviour over more than one year. The novelty lies in the long-term monitoring of embedded urban rail infrastructure using continuously acquired raw data and advanced signal processing and machine learning techniques. Compared with heavy rail, tram operation presents additional challenges due to frequent stop-and-go motion, low operating speeds, external urban noise and numerous infrastructure elements such as switches, crossings and welded joints.

Onboard vibro-acoustic monitoring has been investigated for decades, primarily for heavy-rail applications using axle-box accelerations to detect defects such as corrugation and track irregularities [1], [2], [3]. In contrast, comparatively few studies address tram networks, where operational conditions complicate signal interpretation. Representative examples include acoustic monitoring of wheel-sliding events [4], accelerometer-based assessment of track irregularities [5], [6], and combined onboard and wayside investigations of curve squeal [7]. Recent studies increasingly employ machine learning for onboard condition monitoring, although acoustic data remain considerably less explored than vibration signals [8], [9].

2. Instrumentation and Data Collection

As part of a three-year transnational research project, trams in Austria, Germany and Switzerland were equipped with vibro-acoustic monitoring systems. This study analyses data from three in-service Cityrunner trams operating on Graz's 70 km standard-gauge network. MEMS-microphones were mounted in direct line-of-sight to the wheel–rail contact point, while uniaxial 200 g and triaxial 40 g MEMS-accelerometers were installed on the axle boxes of the front wheels of the central unpowered bogie. The 16-bit microphone sampled at 44.1 kHz captured the audible emission range. Vehicle positions were recorded using 1 Hz

GNSS and mapped onto the network geometry using a georeferencing algorithm. Raw data were retrieved either manually or via LTE. Over a 12-month monitoring period, the instrumented vehicles recorded approximately 68 800 km of data. Temperature, precipitation and humidity data were logged hourly throughout the survey to assess potential weather influences.

Vibro-acoustic data acquisition was velocity-triggered, with all sensor channels recorded at their respective sampling rates while the vehicle was in motion. Owing to the highly variable operating speeds of trams, network coverage was considerably less uniform than in heavy rail. To obtain reproducible condition indices, the network was partitioned into static 5 m sections (bins), representing a compromise between maintenance requirements, georeferencing accuracy and data availability. A relational database stored the bin geometry, the computed vibro-acoustic features, weather data, track properties (e.g. curvature, switches, crossings and superstructure type), known defects and operational parameters such as speed and acceleration.

For each bin, mean and maximum values of approximately 600 features - including sound and vibration levels, third-octave spectra, bandpass levels and corrugation indicators - were calculated and stored for subsequent machine learning analyses. The instrumented fleet was deployed across most of the network to capture diverse operating conditions and seasonal effects.

3. Case study

To illustrate representative trends in the onboard emission levels over the monitoring period, an example track sections is shown here based on its geometric characteristics and maintenance interventions carried out during the survey. The selected section extends from a central interchange through a densely built urban area with narrow streets. The beginning of the section includes several rail crossings, indicated by asterisks in the basemap inset of Figure 1. As the vehicle traverses these rail discontinuities, distinct peaks are observed in the onboard emission data. The impact noise generated by wheel passages across the crossing gaps is particularly evident for the right wheel, where two well-defined clusters correspond to the crossing geometry labelled A and B in the inset.

3.1. Trends over 12 months

The corresponding heat maps illustrate the temporal evolution of sound emissions in the low-frequency third-octave band (with a center frequency of 50 Hz) in Figure 2 and the mid-frequency third-octave band (center frequency 400 Hz) in Figure 3.

Between July and August 2024, a complete rail replacement was carried out between bins 13990 and 14050. The most pronounced change occurred in curve D (bins 14005–14020), where the 50 Hz band exhibited a reduction in onboard emission levels of approximately 10 dB following the intervention. In contrast, the re-

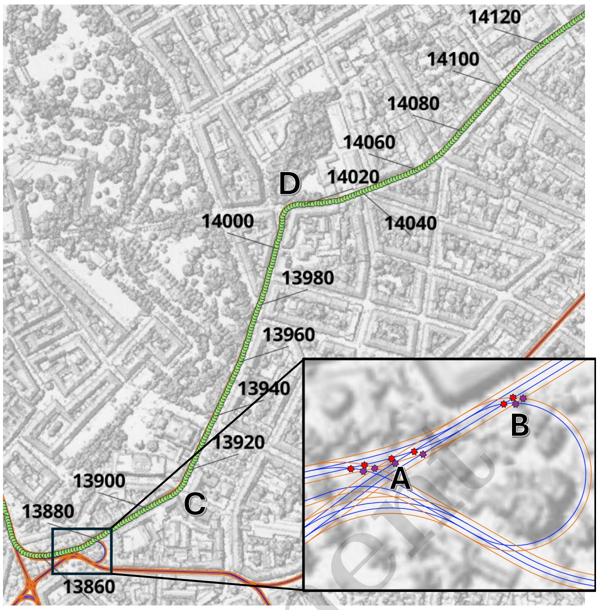

Figure 1: Basemap of the example section showing the track geometry with crossing clusters A and B within the inset and curves C (46 m radius) and D (25 m radius), including bin numbers

placement produced no discernible change in the 400 Hz band, indicating that the maintenance primarily affected low-frequency vibration and noise generation mechanisms.

A characteristic example of curve squeal is observed in curve C, located around bin 13915 in Figure 1. Comparison of the left and right wheel measurements in Figure 3 shows that the elevated sound pressure levels are concentrated predominantly on the inner (left) wheel. The pronounced increase in the 400 Hz band, together with similar features in the 500 Hz band and its higher harmonics, is consistent with stick–slip excitation during curving, leading to the excitation of wheel structural eigenmodes.

In the high-frequency range above 6 kHz, the measured emission levels were found to be strongly influenced by environmental conditions. During periods of precipitation, these frequency bands exhibited substantially elevated sound pressure levels irrespective of track geometry or vehicle speed, suggesting that rolling noise in this range is dominated by broadband splash noise generated at the wheel–rail interface. This behaviour is illustrated in Figure 4 for the third-octave band with a center frequency of 8 kHz..

3.2. Raw data

Heatmaps such as the ones shown above, illustrating the time history of a vibro-acoustic features over consecutive bins, or even network maps, which show the information for a certain point in time along the actual track locations, provide a very helpful overview for decision makers when it comes to highlighting the development or appearance of emission hotspots. Binning is an inevitable form of data aggregation for

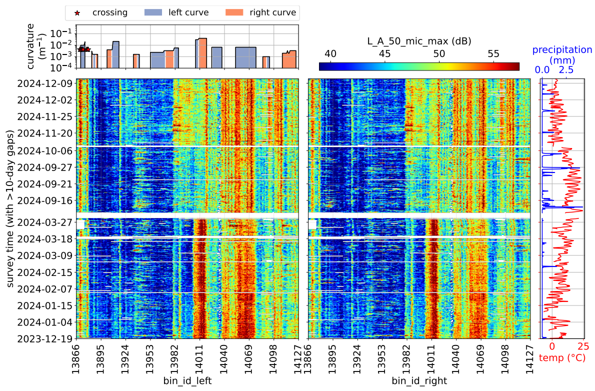

Figure 2: Max. $L_{A,50}$ for each bin along the case study section together with curvature and environment logs

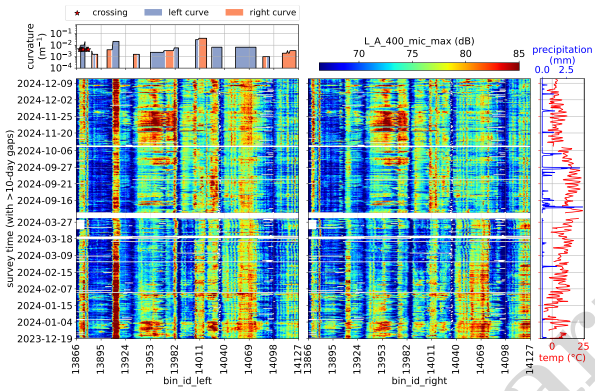

Figure 3: Max. $L_{A,400}$ for each bin along the case study together with curvature and environment logs

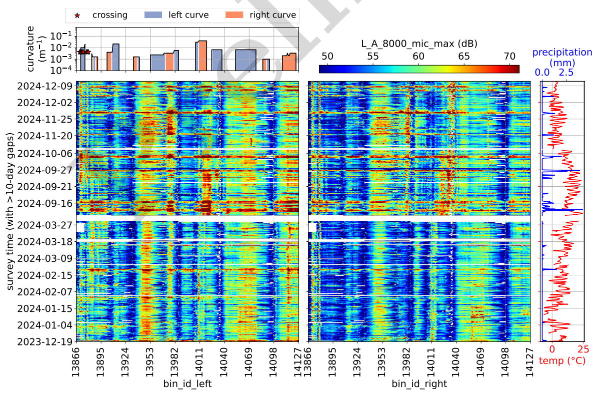

Figure 4: Max. $L_{A,8000}$ for each bin along the case study together with curvature and environment logs

this kind of application, as raw data is impractical to geolocate and costly, given the comparatively low precision level used to mark the start and end points of light rail maintenance (sometime using addresses, landmarks or other verbose descriptions). To show in detail what kind of information is encompassed in the features per bin and how this can vary between different types of rail head irregularity, some raw data examples are shown in this section. The vertical acceleration from the 40 g sensor over 20 m is shown in the following figures, together with the average vehicle speed at the time, when a vehicle passes over

- expansion joints, see Figure 5, characterised by a sudden peak followed by a low-frequency transient;
- crossings after a switch, see Figure 6, characterised by distinct peaks that correspond to the number of gaps in the rails including raised levels just before and after each peak that are indicative of the ramps used in Flange Tip Lift Crossings;
- rail breaks, see Figure 7, also characterised by distinct peaks but of smaller amplitudes compared to crossings and no lead-up to the peaks;
- rail head breakouts, see Figure 8, characterised by continuously high acceleration levels;
- welded joints, see Figure 9, showing up at regular intervals of 15 m and comparatively small peak amplitudes, even at high speeds;
- wayside lubricators, see Figure 10, characterised by similar peak patterns as welded joints but always found before curves.

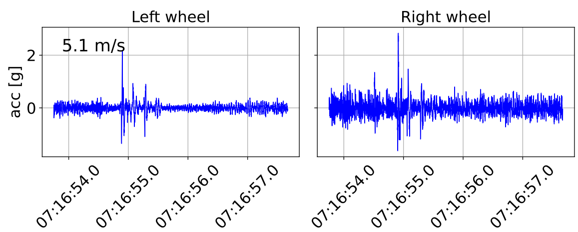

Figure 5: Raw vertical acceleration data of both wheels when driving over an expansion joint

The raw data plots show that for one-sided irregularities, the vibration transfer to the other wheel is minimal, despite the connection via an axle. This suggests that instrumenting both wheels provides the potential to clearly distinguish between defects on the left and right rail.

4. Data preparation for machine learning

A substantial proportion of the measured vibro-acoustic emissions is governed by operational and

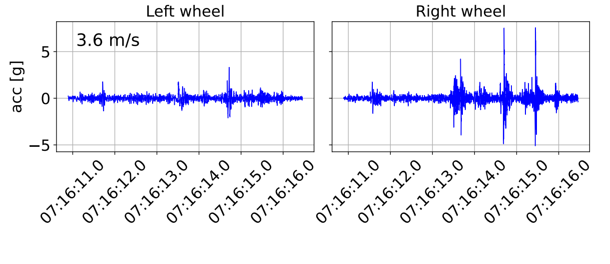

Figure 6: Raw vertical acceleration data of both wheels when driving over crossings (2 gaps along the left rail, 3 gaps on the right rail)

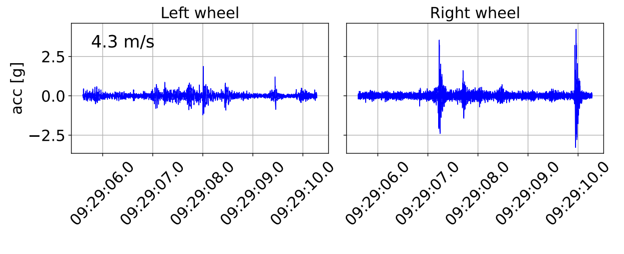

Figure 7: Raw vertical acceleration data of both wheels when driving over rail breaks on the right rail

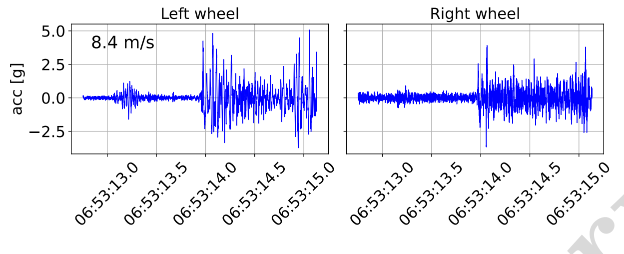

Figure 8: Raw vertical acceleration data of both wheels when driving over an area with strong railhead breakouts

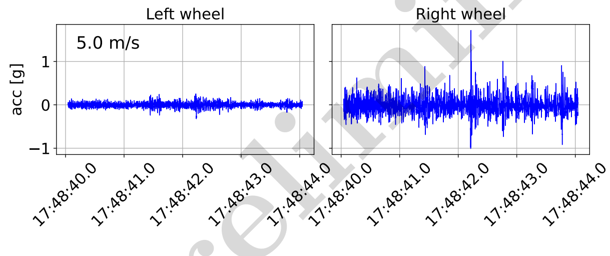

Figure 9: Raw vertical acceleration data of both wheels when driving over a regular weld joint

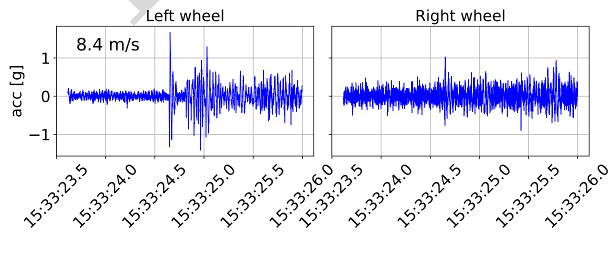

Figure 10: Raw vertical acceleration data of both wheels when driving over a wayside lubricator

environmental factors in addition to the infrastructure condition. To isolate track-related effects and allow for a better detection of potential faults, an ordinary least squares regression model was used to estimate the expected emission level for each feature based on operational parameters such as speed and weather. The coefficients obtained for each independent variable for the total sound pressure level are shown in Table 1 for all three vehicles,

where

$v_{vehicle}$ is the common logarithm of the vehicle speed,

T temperature at the time of the survey,

P precipitation at the time of the survey,

c curvature,

$a_{vehicle}$ the acceleration of the vehicle,

F boolean value of whether the bin contained ≥ 1 crossings and

K a factor for left/right wheel.

Variable	Vehicle 1	Vehicle 2	Vehicle 3
F	3.11	3.45	2.95
K	−0.64	−0.16	−0.15
$v_{vehicle}$	13.11	11.61	10.37
T	0.04	0.01	−0.01
P	0.02	0.23	0.97
c	72.38	114.76	50.27
$a_{vehicle}$	−0.03	0.25	0.30
R^2	0.47	0.36	0.32

Table 1: Coefficients of the linear regression model for the total sound power level $L_{A,sum}$ for the three instrumented vehicles.

Variable	Vehicle 1	Vehicle 2	Vehicle 3
F	9.44	9.66	10.22
K	6.73	3.71	4.79
$v_{vehicle}$	5.37	5.50	3.63
T	0.03	−0.01	−0.03
P	0.94	−0.13	0.21
c	80.99	78.92	107.34
$a_{vehicle}$	0.04	0.53	0.36
R^2	0.47	0.21	0.26

Table 2: Coefficients of the linear regression model for the $L_{Z,sum,40g,z}$ vibration emission levels for the three instrumented vehicles.

The same information for the total vibration level is shown in Table 2. The resulting baseline was subtracted from the measured values, yielding residual emissions that were subsequently analysed using machine learning (ML) techniques.

5. Outlook and current results

In the course of the transnational research project, different machine learning algorithms including sparse dictionary learning and supervised ML were explored to process the onboard vibration and sound data to identify rail surface anomalies and track faults (publications currently under submission).

The data collection is planned to be continued in a follow-up project to investigate the transferability of the results. A first indication of the transferabilty was performed on the Graz dataset, where the models trained on one vehicle were then successfully applied to data from another (similar) vehicle with identical sensor setups. The models were initially employed to differentiate different superstructures along the light rail network that may not be part of a typical geopackage provided by operators. In a second step, models for rail irregularity detection were trained depending on the type of superstructure, to automatically differentiate between different categories of defect that are typically of interest to the network operators. The results are georeferenced datasets, classifying each bin in the network as intact or belonging to one of two possible fault classes to indicate the type of damage most likely encountered according to the vibro-acoustic signature.

6. Acknowledgments

This research was supported by the German Federal Ministry for Transport and Digital Infrastructure (BMVI) within the innovation initiative 'mFUND'.

References

[1] Y. Sato, "Study on high-frequency vibrations in track operated with high-speed trains," *Railway Technical Research Institute, Quarterly Reports*, vol. 18, no. Rpt No. 1013-76, 1977.

[2] M. Molodova, Z. Li, and R. Dollevoet, "Axle box acceleration: Measurement and simulation for detection of short track defects," *Wear*, vol. 271, no. 1, pp. 349–356, 2011, Proc. of the 8th International Conference on Contact Mechanics and Wear of Rail / Wheel Systems, Florence, 2009, ISSN: 0043-1648. DOI: https://doi.org/10.1016/j.wear.2010.10.003

[3] K. Zhang and X. Liu, "Identification of rail corrugation in high-speed railway using vmd-spwvd," *KSCE Journal of Civil Engineering*, vol. 30, no. 2, p. 100 363, 2026, ISSN: 1226-7988. DOI: https://doi.org/10.1016/j.kscej.2025.100363

[4] W. Xie, A. Nunez, R. Maas, and Z. Li, "Decision support tool based on multi-source data analysis for the tram wheel-rail interface," *IFAC-PapersOnLine*, vol. 51, no. 9, pp. 118–123, 2018, 15th IFAC Symp. on Control in Transportation Systems CTS 2018, ISSN: 2405-8963. DOI: https://doi.org/10.1016/j.ifacol.2018.07.020

[5] Á. Vinkó and P. Bocz, "Experimental investigation on condition monitoring opportunities of tramway tracks," *Periodica Polytechnica Civil Engineering*, vol. 62, no. 1, pp. 180–190, 2018. DOI: https://doi.org/10.3311/PPci.10541

[6] Y. D. Jelila and W. Pamuła, "Application of mems sensors for the condition monitoring of urban tramways based on MODWPT," *IEEE Sensors Journal*, vol. 23, no. 20, pp. 24 300–24 307, 2023. DOI: 10.1109/JSEN.2023.3309648

[7] F. Castellini et al., "Experimental and numerical investigation of tramcar curve squeal under varying wheel-rail contact conditions," *Computers & Structures*, vol. 321, p. 108 040, 2026, ISSN: 0045-7949. DOI: https://doi.org/10.1016/j.compstruc.2025.108040

[8] A. Ji, W. L. Woo, E. W. L. Wong, and Y. T. Quek, "Rail track condition monitoring: A review on deep learning approaches," *Intelligence & Robotics*, vol. 1, no. 2, 2021, ISSN: 2770-3541. DOI: 10.20517/ir.2021.14

[9] X. Mao et al., "Acoustic vibration characteristics for combined diagnosis of rail corrugation: An application of mcissa and permutation heterogeneous recurrence plot," *Results in Engineering*, vol. 29, p. 109 464, 2026, ISSN: 2590-1230. DOI: https://doi.org/10.1016/j.rineng.2026.109464